Long-Term Behaviour and Environmentally Friendly Rehabilitation Technologies of Dams (LTBD 2017) DOI:10.3217/978-3-85125-564-5-082

Field Seepage Tests on Discontinuity Structural Rocks in a Hydropower Project

Sihong Liu[1], Bin Zhou1, Liping Weng[2], Meiqi Jiang[3], Hanwen Xiong[4]

1-College of Water Conservancy & Hydropower Engineering, Hohai University, Nanjing 210098, China
2- Business school of Hohai University, Nanjing 210098, China
3-Zhejiang Hua Dong Construction Engineering Co., LTD, Hangzhou 310000, China
4-Water Resources Pearl River Planning Surveying & Designing Co., LTD, Guangzhou 510000, China

Email: sihongliu@hhu.edu.cn

Abstract

The permeability characteristics of the structural planes inside rock masses are of importance for the stability of hydropower station projects. In this paper, a large-scale in-situ seepage testing method was proposed and applied to the tests on the gently dipping structural plane (C2 zone) and the steep fault (F14) in the construction field of one hydropower station in China. The in-situ test results were compared with those of both the undisturbed and the reconstituted specimens. The test results indicate that the proposed in-situ testing method can be effectively used to determine the permeability characteristics of structural planes under the natural stresses with a relatively high accuracy. The critical hydraulic gradient of the structural planes is influenced by the natural stress of the surrounding rock mass, which cannot be reflected in the tests on the undisturbed and the reconstituted specimens.

Keywords: In-situ seepage test, permeability characteristic, rock discontinuity structural plane.

1. INTRODUCTION

The Baihetan project, located on Jinsha River and with a total installed capacity of 1,600 megawatts, is the second largest hydropower station currently under construction in China. A concrete double-curvature arch dam with a height of 289 m will be built. The Emeishan basalt rocks, in which many rock discontinuities such as the bedding fault zones, small faults and fractures, spread over the dam site, as shown in Fig.1. According to their inclinations, the rock discontinuities can be roughly classified into the gentle-dip bedding fault zones and the steep faults.

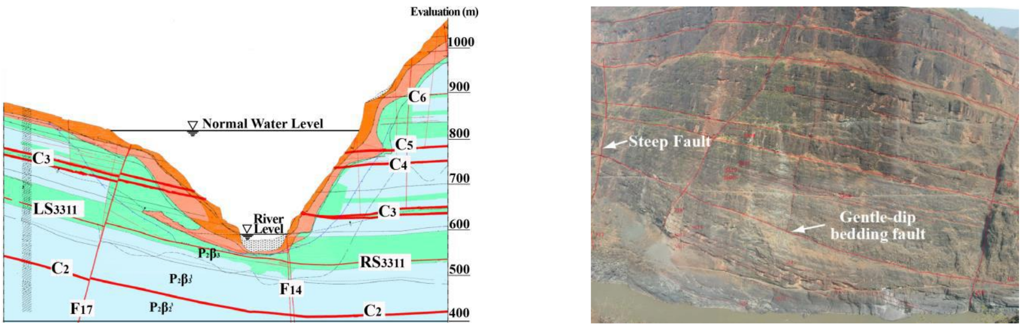

(a) Geological profile along the dam axis (b) Photo of rock discontinuities

Fig.1 Rock discontinuities at the dam site of Baihetan project

Before the construction, most of the rock discontinuities are well above the groundwater or river level. After the completion of the project and the impounding of the reservoir, the water pressure within the rock discontinuities will significantly increase, resulting in the following two adverse effects on the project. One is the leakage of the reservoir water through the rock discontinuities; the other is the possibility of seepage deformation failures of the rock discontinuities and the subsequent failure of the dam foundation as well as the abutments. Therefore, the hydraulic properties of the rock discontinuities are crucial to the safety of the Baihetan project.

At present, the hydraulic properties of rock discontinuities are mainly determined through laboratory or field seepage tests and borehole water pressure tests. For laboratory tests, the sampling in the field will inevitably disturb the rock discontinuities and the reliability of the test results depends on the specimen size and the sampling location. The small specimen will not be representative, and the large specimen will be difficult to be handed [1][2]; Borehole water pressure tests [3] are usually conducted in the boreholes with a depth of at least 5m and the test results reflect the average permeability of the fractured rock mass in a relatively wide range; The field seepage tests, usually conducted in adits, are probably the best approaches for investigating the hydraulic properties of rock discontinuities [4][5]. There are some reports on field seepage tests [6][7].

In this paper, we introduce a new in-situ seepage testing method for rock discontinuities, in which the stress environment of the specimen is closer to the natural situation and the specimen is more representative of rock discontinuities. The application examples in Baihetan dam site are presented.

2. PRINCIPLE OF IN-SITU SEEPAGE TEST

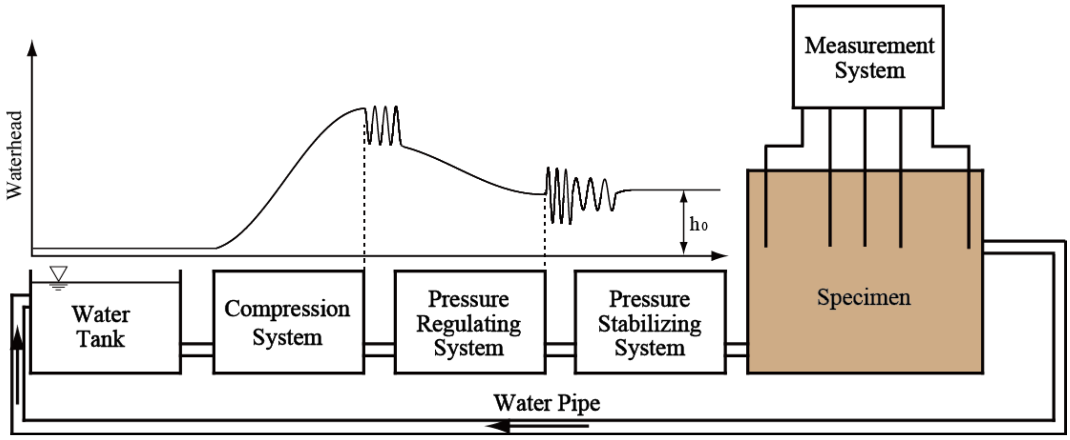

Fig.2 Principle of the in-situ seepage test

Fig.2 shows the principle of the new in-situ seepage tests on rock discontinuities. It consists of the water supply, the compression, the pressure regulating, the pressure stabilizing and the measurement systems. Through the compression system, the head of the water from a tank is raised to the rated maximum value of the centrifugal pump used in the test. Then, by means of the pressure regulating and the pressure stabilizing systems, the water head is regulated to a preset value h_0 at the inlet of the specimen. When the pressurized water flows through the specimen, the water temperature is recorded and the change of the water pressure within the specimen are measured with five piezometric tubes. The water flowing out of the specimen goes back to the tank through a pipe, achieving the cyclic utilization of the water. The inlet water pressure is gradually increased and applied onto the specimen through the pressure regulating and the pressure stabilizing systems. At one inlet water pressure, the measurement continues until the outlet flow per unit time reaches a stable value.

Figs.3 and 4 show the schematic views on gentle-dip bedding fault zones and steep faults, respectively. The tests are carried out in adits. Since the protolith surrounded the rock discontinuities is the compact and slightly weathered or fresh tuff in this project, it is considered to be nearly impermeable. For the gentle-dip bedding fault zones, the upper and lower parts of the specimen are the protolith and the two lateral sides (the inlet and the outlet) of the specimen are surrounded by the reinforced concretes (about 50cm thick). To prevent the contact leakage between the reinforced concretes and the specimen, a layer of plastic clay (about 5cm thick) is placed on the two side surfaces of the specimen before casting the reinforced concrete. For the deep faults, the two lateral sides of the specimen are the protolith and upper and lower parts of the specimen are isolated with reinforced concretes. The inlet and outlet of the specimen are sealed with reinforced concretes. Between the reinforced concretes and 3 the specimen, the 30cm thick filter of sandy pebbles (the maximum gain size d_{max}=2cm) is placed to prevent the damage of the specimen by the pressurized water.

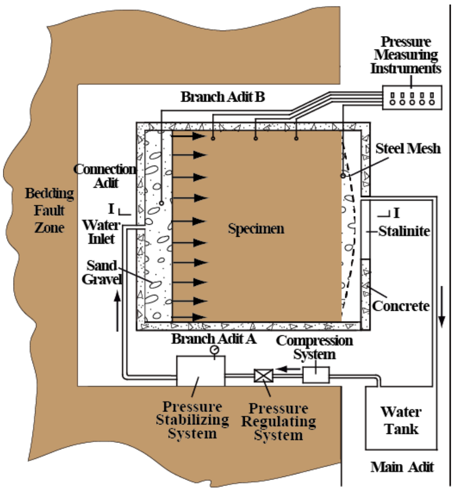

(a) Plan view

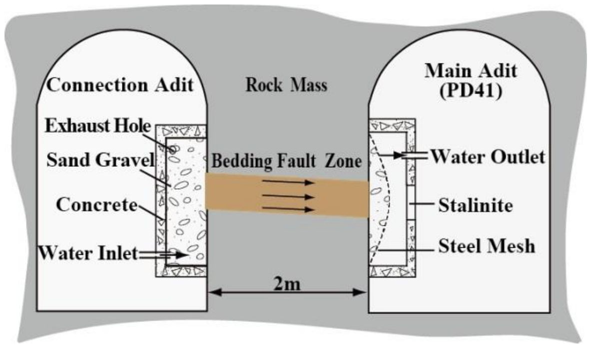

(b) I-I section

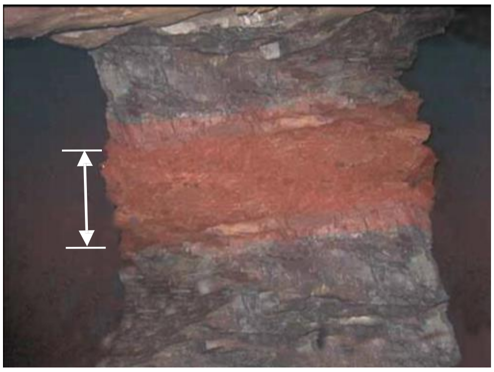

(c) YS1 specimen

(d) Completion of the in-situ specimen

Fig.3 Schematic of in-situ seepage test on gentle-dip bedding fault zones

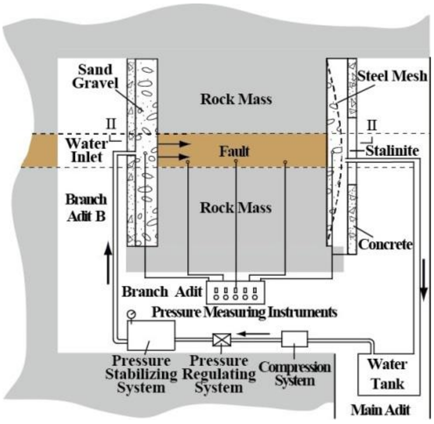

(a) Plan view

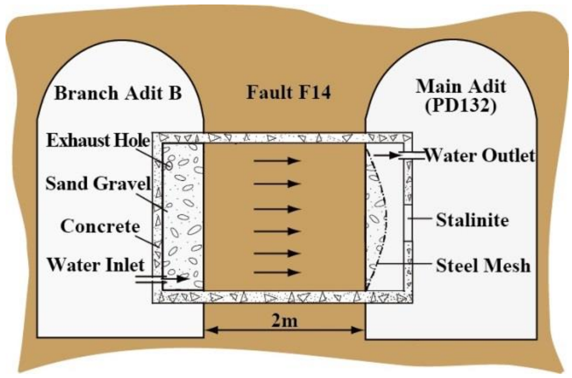

(b) II-II section

Fig.4 Schematic of in-situ seepage test on steep faults

3. APPLICATION EXAMPLES

Two application examples of the in-situ seepage tests on the gentle-dip bedding fault zone (C_3) and on the steep fault (F_{14}) in Baihetan dam site, respectively, are presented. The test procedures mainly include the specimen preparation, the specimen saturation, the seepage pressure application and the data acquisition. They are almost the same for the two application examples except the specimen preparation as illustrated in Figs.3 and 4.

The bedding fault zone (C_3) is palm red and has an average thickness of about 26 cm. It is the fractured tuff zone and filled with gravels, debris and some mud, with a natural void ratio ranging from 0.25 to 0.39. The filling materials within the bedding fault zone (C_3) has a good gradation with the characteristics of d_{max}=60mm, d_{50}=0.1mm and C_u=60. The in-situ specimen of the gentle-dip bedding fault zone (C_3), denoted as YS1, has a seepage length of 200cm and a seepage section of 200cm×26cm, as shown in Fig.3.

The steep fault (F_{14}) is basically a fractured rock with breccia and gravels contained in its voids, and has an average width of 43cm. It is in a relatively dense state with a natural void ratio of about 0.15. The grains contained in F_{14} are relatively uniform with a coefficient uniformity C_u=4. Their grain sizes mainly range from 4mm to 30mm and the fine grains (d<0.1mm) contained in F_{14} are less than 5%. The prepared specimen of the steep fault (F_{14}), denoted as YS2, has a seepage length of 200cm and a seepage section area of 200cm high by average 45cm wide.

During the test, the seepage flux and the water heads at five piezometric tubes as well as the water temperature at the outlet chamber were measured every half an hour. Meanwhile, all phenomena, such as the turbidity and the bubbling within the seepage flow, and the suspension of the entrained fine particles in the outlet chamber, etc., were closely observed and timely recorded. The hydraulic gradient *i* and the seepage velocity *v* of the specimen at each staged pressure were calculated from the measurements of the water heads and the seepage flux. The hydraulic conductivity of the specimen at the test temperature was obtained from the Darcy's law and then converted to the equivalent one at a temperature of 20℃ (denoted as k_{20}), expressed as:

$$k_T = \frac{v}{i}, \quad k_{20} = k_T \frac{\eta_T}{\eta_{20}} \qquad (1)$$

where and are the coefficients of water dynamic viscosity at the test temperature T℃ and 20℃, respectively.

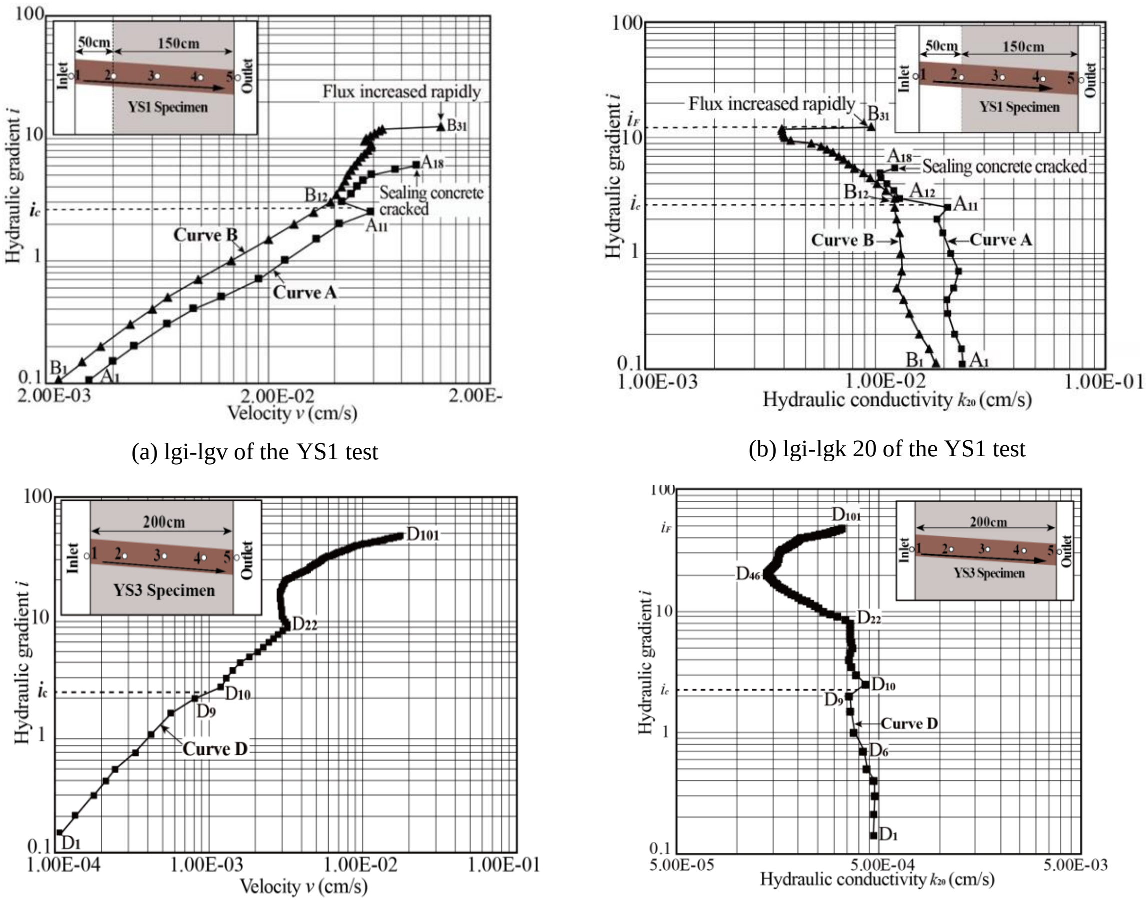

(a) lgi-lgv of the YS1 test

(b) lgi-lgk 20 of the YS1 test

(c) lgi-lgv of the YS2 test

(d) lgi-lgk20 of the YS2 test

Fig.5 Results of the YS1 and YS2 tests

Fig.5 gives the results of the two tests with respect to the change of hydraulic gradient with the seepage velocity and the hydraulic conductivity in double logarithmic coordinates. The YS1 test was repeated twice because some cracks took place in the sealing concretes surrounding the specimen during the test. In YS1 test, very small hydraulic gradients had been measured between the piezometric tubes 1 and 2, indicating that the fractures may be well developed and the seepage channel is interconnected near the inlet chamber. Therefore, the hydraulic gradients in Figs.5(a) and (b) were obtained from the measurement of the piezometric tubes 2 and 5 as well as the corresponding seepage length. In Figs.5(a) and (b), the curves A and B represent the twice results of the YS1 test before and after the reinforcement of the sealing concrete of the specimen, respectively. Along the curve A in Fig.5(a), the hydraulic gradient i increases almost linearly with the seepage velocity v from points A_1 to A_{11}. At point A_{11}, the hydraulic gradient i is 2.5. When the hydraulic gradient i increases from 2.5 to 3.0 (point A_{11} to point A_{12}), the seepage velocity v decrease slightly, indicating that the possible change of the internal structure of the specimen happens and some fine particles start to move along the seepage direction. The average value of the hydraulic gradients at points A_{11} and A_{12} could be regarded as the critical hydraulic gradient i_c, which is equal to 2.75. After the point A_{12}, the hydraulic gradient i increases further with the seepage velocity v until it reaches 6.0 at point A_{18}, where the cracking of the sealing concrete of the specimen happened and the test had to be stopped. From Fig.5(b), it can be seen that the hydraulic conductivity of the YS1 specimen changes slightly (ranging from 0.018 cm/s to 0.023 cm/s) before the point A_{11}. After the point A_{11}, the hydraulic conductivity decreases due to the increase of the fine particles along the seepage path. At the point A_{18}, the hydraulic conductivity increases suddenly as the cracking of the sealing concrete of the specimen happened.

As shown in Figs.5(a) and (b), the evolution of the curve B is similar to that of the curve A for the YS1 specimen. However, both the seepage velocity and the hydraulic conductivity in the curve B are slightly smaller than those in the curve A under the same hydraulic gradient because the partial seepage channel is blocked by the fine particles in the repeated test. When the hydraulic gradient i reached 12.50 at the point B_{31}, the seepage flow increased rapidly and it was observed that plenty of fine particles flowed out of the specimen in the outlet chamber. Therefore, the average value of the hydraulic gradients at points B_{30} and B_{31} was regarded as the failure hydraulic gradient i_F, which is equal to 12.25.

As the internal structure of the specimen may have changed after the critical hydraulic gradient i_c, the hydraulic conductivity of the specimen should be taken the value before i_c is reached. Thus, the hydraulic conductivity of the YS1 specimen should be taken from the curve A in Fig.5(b), which is about 2.13E-02cm/s by averaging the values from points A_1 to A_{11}.

For the YS2 specimen, it can be seen from Fig.5 (c) that the hydraulic gradient i increases almost linearly with the seepage velocity v from points D_1 to D_9. During the YS2 test, it was observed that the water level in the inlet chamber began to fluctuate and the seepage flow increased slightly when the hydraulic gradient reached 2.0 at point D_9. When the hydraulic gradient increased from 2.0 to 8.5 (from points D_9 to D_{22}), some fine particles flowed out of the YS2 specimen and the seepage water became turbid. However, the seepage water gradually changed from turbid to clear, together with the decrease of the seepage flow, from the points D_{22} to D_{46}, indicating that the fine particles flowing out of the specimen decreased and a new stable state of the internal 6.

Structure was achieved inside the specimen. After then, the further increase in the hydraulic gradient resulted in the movement of the fine particles again. When the hydraulic gradient reached 48.0 at point D_{101}, the water level in the inlet chamber varied greatly and plenty of fine particles flowed out of the specimen with a sudden increase of the seepage flow, leading to the seepage failure of the specimen.

As the fine particles began to move at point D_9 with a pronounced change of the slopes of both the lg$i$-lg$v$ and the lg$i$-lgk_{20} curves in Figs.5(c) and (d), the critical hydraulic gradient of the YS2 specimen was taken as the average value 2.25 at the points D_9 and D_{10}. Accordingly, the hydraulic conductivity k_{20} was taken as the average value before the point D_9, i.e. 4.23E-4cm/s. The failure hydraulic gradient of the YS2 specimen was taken as the average values at the points D_{100} and D_{101}, which was equal to 47.75.

The hydraulic properties of rock discontinuities are comprehensively influenced by their voids, grain sizes, gradations and so on. Usually, it is considered that the internal structure of the specimen starts to change when the hydraulic gradient reaches its critical one. As the filling materials within YS2 specimen are relatively uniform with a coefficient uniformity C_u=4 and the content of fine particles ($d<0.1$mm) is less than 5%, the skeleton pores formed by coarse particles cannot be fully filled with fine particles. Consequently, fine particles are more likely to migrate in the skeleton pores under seepage pressures, leading to a lower critical hydraulic gradient compared with YS1 specimen. As the natural void ratio of the filling materials in YS1 specimen is larger than that of YS2 specimen, it is easy to understand that the hydraulic conductivity of YS1 specimen is larger than that of YS2 specimen.

By the way, the measured seepage velocities v at point A_{18} and D_{101} are 0.098cm/s and 0.0177cm/s, respectively. The Reynolds numbers R_e of the YS1 and YS3 specimens were calculated to be 86.21 and 15.53, respectively, on the assumption that the kinematic viscosity of water equals to m2/s, illustrating that the seepage flow both in YS1 and YS3 specimens is laminar flow and the Darcy's law holds. 1.31E-06

4. CONCLUSIONS

In this study, an in-situ seepage testing method for large-scale rock discontinuities was introduced. It consists of the water supply, the compression, the pressure regulating, the pressure stabilizing and the measurement systems. In this testing method, the stress environment of the in-situ specimen is closer to the natural situation and the large-scaled specimen is more representative of rock discontinuities.

This new in-situ seepage testing method was firstly applied in Baihetan dam site. The determination of the in-situ specimen dimensions to be representative of rock discontinuities should be further studied. Also, the testing procedures and devices for this new method should be standardized.

5. ACKNOWLEDGEMENTS

The authors gratefully thank the anonymous reviewers for their kind efforts and valuable comments in improving this study. Special thanks are extended to Xu Jianrong, Tang Mingfa, Wang Xuyun, and Xu Gaofeng of Power China Huadong Engineering Corporation for their valuable discussion and great supports.

6. REFERENCES

1. Nastev, M., Savard, M.M., Lapcevic, P. (2004). "Hydraulic properties and scale effects investigation in regional rock aquifers, southwestern Quebec, Canada." Hydrogeology J., Vol.12, pp.257-269.
2. Zhang, W., Chen, J.P., Liu, C., Huang, R., Li, M., Zhang, Y. (2012). "Determination of geometrical and structural representative volume elements at the Baihetan dam site." Rock Mech. Rock Eng., 45(3), pp.409-419.
3. Hsieh, P.A., Neuman, S.P. (1985). "Field determination of the three-dimensional hydraulic conductivity tensor of anisotropic media." Water Resource Research, Vol.21, pp.1655-1665.
4. Cosenza, P., Ghoreychi, M., Bazargan-Sabet, B., De Marsily, G. (1999). "In-situ rock salt permeability measurement for long term safety assessment of storage." Int. J. Rock Mech Min Sci., 36(4), pp.509-526.
5. Cook, P. (2000). "In-situ pneumatic testing at Yucca Mountain." Int. J. Rock Mech Min Sci., 37, pp.357-367.
6. Zhou, Z.F., Yang, J., Yang, H. (1999). "A field test method for determining permeability parameters of gently dipping structural face in rock mass." Journal of Engineering Geology 7, pp.375-379.
7. Feng, S.R., Zhao, H.B., Jiang, Z.M. (2012). "Experimental study on seepage failure characteristics of broken rock mass in dam foundation at left bank of Xiangjiaba Hydropower Project." Chinese Journal of Geotechnical Engineering, 34, pp.600-605.